Dalton Transactions

ROYAL SOCIETY OF CHEMISTRY

PAPER

View Article Online
View Journal | View Issue

Cite this: *Dalton Trans.*, 2023, **52**, 12341

Trinitromethyl-triazolone (TNMTO): a highly dense oxidizer†

Sohan Lal, [a] Richard J. Staples [b] and Jean'ne M. Shreeve *[a]

Received 15th July 2023,
Accepted 8th August 2023

DOI: 10.1039/d3dt02232c

rsc.li/dalton

A scalable synthesis of 5-(trinitromethyl)-2,4-dihydro-3*H*-1,2,4-triazol-3-one (**TNMTO**) is possible from commercially available 2-methylpyrimidine-4,6-diol. It exhibits high density (1.90 g cm^{-3}) with comparably low thermal stability (T_d = 80 °C) and positive oxygen balance (OB^{CO} = 20.51%, OB^{CO_2} = 0.0%). **TNMTO** has an attractive combination of detonation properties (P = 35.01 GPa, D = 8997 ms^{-1}) and propulsive properties ($I_{sp(neat)}$ = 251.85 s, $\rho I_{sp(neat)}$ = 478.52 gs cm^{-3}, $C^*_{(neat)}$ = 1501 ms^{-1}). These are superior to ammonium dinitroamide (ADN), 2,2,2-tetranitroacetimidic acid (TNAA) and ammonium perchlorate (AP), making it a potential green oxidizer in solid rocket propulsion.

1. Introduction

Solid propellant, a composition of propellant/fuel, binder, plasticizer, oxidizer, and curing agents, is a new emerging field in high energy density materials (HEDMs).[1,2] These materials produce excellent propulsive thrust by generating high-temperature gaseous products upon deflagration during combustion. Many research groups contribute to developing novel solid propellants by designing their core components, such as propellants/fuel, binders, plasticizers, oxidizers, and curing agents. However, the two most important components of solid propellants are the fuel and oxidizer. In the last few decades, ammonium perchlorate-based (AP) composite propellants (with GAP/HTPB/Al) have been extensively studied in space-related applications. Ammonium perchlorate (AP) has an excellent oxygen balance (34%) with a high density (ρ = 1.95 g cm^{-3}) and is very frequently used as an oxidizer to produce the best thrust in rocket propulsion systems.[3] However, it produces extremely toxic gaseous products (HCl, Cl_2, NO, N_2O, *etc.*) during combustion, continuously contaminating the environment.[4] Therefore, this is the ideal time to develop an improved oxidizer for rocket propulsion. Recently, some interesting green oxidizers (chlorine free), namely bis(3-nitro-1-(trinitromethyl)-1*H*-1,2,4-triazol-5-yl) methanone (**BNTNMTMO**, **1**),[5] 4,4′,5,5′-tetranitro-2,2′-bis-(trinitromethyl)-2*H*,2′*H*-3,3′-bipyrazole (**TNBTNMBP**, **2**),[6] 1,3-dinitro-6-(trinitromethyl)-1,2,3,4-tetrahydro-1,3,5-triazine (**DNTNMTHT**, **3**),[7] (*Z*)-*N*,2,2,2-tetranitroacetimidic acid (**TNAA**, **4**),[8] and 5-azido-10-nitro-1*H*,5*H*-bis(tetrazolo)[1,5-*c*:5′,1′-*f*]-pyrimidine (**ANBTzP**),[9] have been developed, which have shown potential for replacing AP since they exhibit excellent energetic properties as oxidizers are listed in Fig. 1. On the other hand, ammonium dinitramide (ADN)[10] and hydrazinium nitroformate (HNF)[11] are well-known chlorine-free energetic materials; however, they also have some drawbacks, including their high negative enthalpies of formation, high sensitivities, and hygroscopic nature. Nitrotrizolone (**NTO**, **5**) was synthesized a century ago, and is a unique molecule that has many desirable features, including high density, high detonation velocity, and pressure with its unexpected insensitivity toward the mechanical stimulus, which makes it an interesting energetic material. Thus, it has been extensively utilized in munitions.[12] Recently, we have reported some different analogues of NTO.[13] In a continuing effort to explore its chemistry, our goal has been to synthesize novel high-energy-density materials (oxidizers, propellants, and explosives) with excellent properties. In the series of new oxidizers,

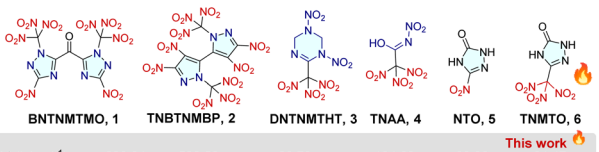

$\Delta H_f°$ (kJmol^{-1})	=	-623.94	522.50	-60.70	-134.60	-68.30	-64.47
N+O (%)	=	84.77	84.30	83.93	89.53	79.98	83.74
P (GPa)	=	28.60	40.00	38.10	23.00	30.90	35.01
D (km/s)	=	8252	9320	9112	7503	7992	8997
ρ (g/cm^3)	=	1.93	2.02	1.87	1.87	1.93	1.90
T_d (°C)	=	164	125	141	137	254	80
IS (J)	=	≥9	≥9	≥6	≥19	≥22	≥10
Isp_{neat} (s)	=	219	254	258	209	218	252

Fig. 1 Representative oxidizers with trinitro-methyl ($-C(NO_2)_3$) moieties[5–8] and NTO.[12]

[a]*Department of Chemistry, University of Idaho, Moscow, Idaho, 83844-2343, USA. E-mail: jshreeve@uidaho.edu; Fax: (+1) 208-885-5173*
[b]*Department of Chemistry, Michigan State University, East Lansing, Michigan 48824, USA*

†Electronic supplementary information (ESI) available. CCDC numbers are 2268205–2268207. For ESI and crystallographic data in CIF or other electronic format see DOI: https://doi.org/10.1039/d3dt02232c

we now report the synthesis of **TNMTO**, **6** as a green and highly dense oxidizer with balanced performance for rocket propulsion.

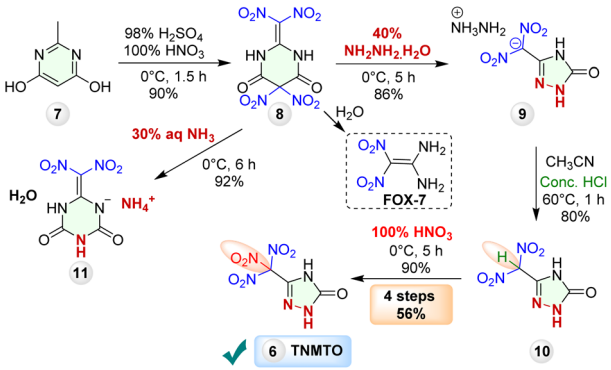

Scheme 1 Synthesis of **TNMTO**.

2. Results and discussion

2.1. Synthesis

Commercially available 2-methylpyrimidine-4,6-diol **7**, which was first nitrated with a 1 : 1 nitrating mixture (98% H_2SO_4 and 100% HNO_3) at 0 °C to isolate pure compound **8**,[14] for the first time, in pure form. Subsequently **8** was treated with hydrazine (40% solution in H_2O) to give **9** in excellent yield. Then **9** under acidic conditions (12 M HCl) formed 5-(dinitromethyl)-2,4-dihydro-3*H*-1,2,4-triazol-3-one **10**[13] in excellent yield. Finally, compound **10** was further nitrated with 100% HNO_3 to give 5-(trinitromethyl)-2,4-dihydro-3*H*-1,2,4-triazol-3-one (**TNMTO**, **6**) as shown in Scheme 1. When compound **8** was treated with aqueous NH_3 (30% solution), excellent yields of **11** resulted. Its structure was confirmed by single crystal X-ray analysis.

2.2. Crystal structure

Compound **8** yields FOX-7[15] on hydrolysis (see Fig. S24 and S25, ESI†). **TNMTO** (**6**) was crystallized by slow recrystallization

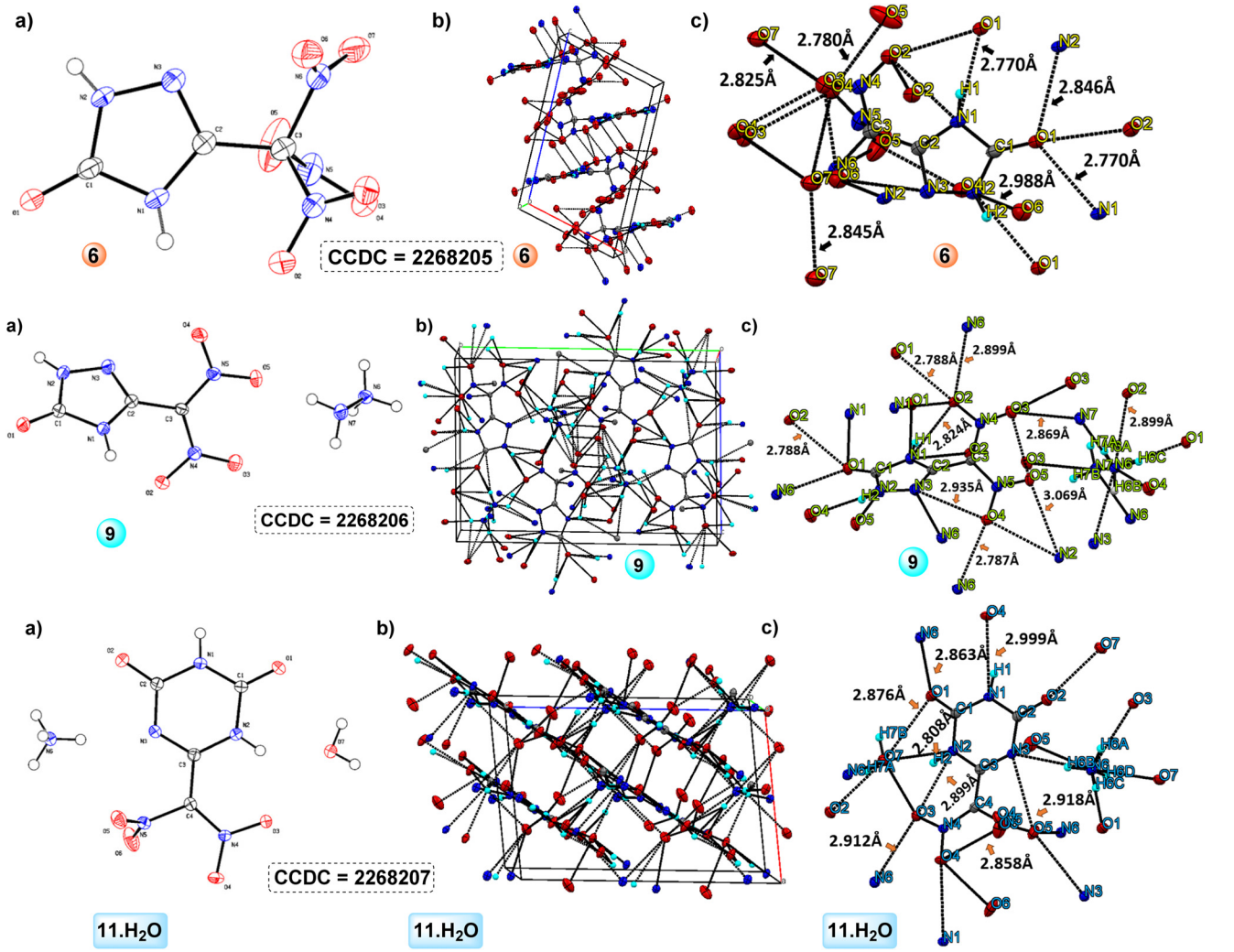

Fig. 2 (a) Single crystal X-ray structure; and (b) packing diagram; (c) H-bonds of compounds **6**, **9** and **11**·H_2O.

from DCM and exhibits a monoclinic *P*21/*n* space group. Its crystal density is 1.902 g cm^{-3} at 100 K with a single molecule in the asymmetric unit (Z = 4, Z' = 1), as seen in Fig. S5–S9 (see ESI†). **TNMTO** crystals have a network of intermolecular H-bonds and π–π-interactions, which contribute to the higher density of 1.902 g cm^{-3} at 100 K and an experimental density of 1.900 g cm^{-3} at 25 °C. The C–C bond length (C2 = C3 = 1.484 Å) for compound **TNMTO** is slightly shorter than TNAA (C1 = C2 = 1.534 Å). The torsion angle of N3–C2–C3–N4 is 136.6°, N3–C2–C3–N5 is 103.8°, N3–C2–C3–N6 is 14.4° and that of N1–C2–C3–N4 is 49.9°, N1–C2–C3–N5 is 69.7°, N1–C2–C3–N6 is 172.09° suggesting that the molecule is rigidly packed (Fig. 2). The H-bonding interplay has a maximum 3.1 Å D–D distance and a minimum 110° angle present in **TNMTO**: N1–O1: 2.77 Å, N2–O1: 2.846 Å, N2–O6: 2.988 Å, O3–O7: 2.825 Å.

Compound **9** was crystallized by slow recrystallization from CH_3CN and exhibits a monoclinic *P*21/*n* space group (see Fig. 2 and Table S11, ESI†). Compound **11** was crystallized by slow recrystallization from CH_3CN and exhibits a monoclinic *P*21/*n* space group (see Fig. 2 and Table S12, ESI†).

2.3. Physicochemical properties

The enthalpy of formation $\left(\Delta H_f^\circ(s)\right)$ of **TNMTO** was estimated using Gaussian 03 suite of programs[18] with the help of the isodesmic method (see Table 1 and Fig. S1, ESI†). Subsequently, corresponding detonation and propulsive performances were evaluated with $\left(\Delta H_f^\circ(s)\right)$ and experimental densities by using EXPLO5 V6.06 software.[19] **TNMTO** exhibits a negative $\Delta H_f^\circ(s)$, −64.47 kJ mol^{-1}. However, it is superior to TNAA (−134.60 kJ mol^{-1}), AP (−295.80 kJ mol^{-1}), and ADN (−134.60 kJ mol^{-1}). Oxygen balance (OB, Ω), the degree to which all hydrogen can be converted to H_2O and all carbon into CO or CO_2, is listed in Table 1. **TNMTO** has a high positive OB at 20.51% with a high density of 1.900 g cm^{-3}, comparable to well-known oxidizers TNAA and ADN. The efficiency of fuels/propellants can be measured in terms of their specific impulse (I_{sp}). The propulsive power of **TNMTO** was evaluated at two different compositions (i) neat compound, and (ii) composite formulation with aluminium (Al). Results revealed that, as a neat compound, **TNMTO** exhibits a propulsive power superior to that of TNAA, ADN, AP, K_2BDAF and K_2DNABT. While in the composite formulation, it performed better than TNAA, K_2BDAF, AP, ADN and illustrate slightly lower density specific impulse (ρI_{sp}) than K_2DNABT (Table 1 and Fig. 3).

Mulliken's charges are shown in Fig. 4, C3–C18 is the most polar bond and N14 is the most negatively charged N-atom in the molecule.

The electrostatic potentials (ESP) of **TNMTO**, **6** were analysed by B3LYP/6-311++G(d,p) method and plotted with Multiwfn and VMD software.[20] the negative fraction (blue) and a positive fraction (red) located on nitro groups and triazolone ring, respectively and indicate the comparatively more and less active sites on the molecule surface (Fig. 5a).

Since ESP gives the indication of impact sensitivity, the high electron availability (more negative ESP surface), resulted

Table 1 Comparison of physicochemical properties of **TNMTO**, **TNAA**, **AP**, **ADN**, **K_2BDAF** and **K_2DNABT**

Compound	**TNMTO, 6**	**TNAA**[a]	**AP**[b]	**ADN**[c]	**K_2BDAF**[d]	**K_2DNABT**[e]
Formula[f]	$C_3H_2N_6O_7$	$C_2HN_5O_9$	NH_4ClO_4	$NH_4N(NO_2)_2$	$C_6K_2N_{10}O_{10}$	$C_2K_2N_{12}O_7$
FW(g mol^{-1})[g]	234.08	238.98	117.49	124.06	450.30	334.30
Ω^{CO} (%)[h]	20.51	43.50	34.04	25.80	10.66	14.35
Ω^{CO_2} (%)[i]	0.0	30.12	27.23	25.80	−7.10	−4.8
O (%)[j]	48	60	54	45	36	19
N + O (%)[k]	83.74	89.53	66.39	96.75	66.63	69.42
ΔH_f (kJ mol^{-1})[b,l]	−64.47	−134.60	−295.80	−149.72	110.10	326.40
ρ (g cm^{-3})[c,m]	1.90	1.87	1.95	1.81	2.04	2.11
T_d (°C)[n]	80	137	200	159	229	200
P (GPa)[o]	35.01	23.00	15.80	23.60	30.10	31.70
D (ms^{-1})[p]	8997	7503	6368	7860	8138	8330
$-Q$ [kJ kg^{-1}][q]	5626	3215	1435	2754	5514	4959
IS (J)[r]	≥10	≥19	≥15	3–5	≥2	≥1
FS (N)[s]	≥120	≥20	≥360	64–72	≥20	≤1
BDEs (kJ mol^{-1})[t]	58.15	102.11	—	—	—	—
Φ_{H-L} (eV)[u]	3.549	5.385	—	—	—	—
I_{sp} (s)[v,aa]	251.85	208.61	156.63	202.14	227.26[ab]	210.49[ab]
ρI_{sp} (gs cm^{-3})[w,aa]	478.52	390.11	305.43	365.87	463.61[ab]	444.13[ab]
C^* (ms^{-1})[x,aa]	1501	1289	977	1267	1398[ab]	1258[ab]
I_{sp} (s)[y,aa]	258.58	241.32	232.00	256.25	242.39[ab]	239.17[ab]
ρI_{sp} (gs cm^{-3})[z,aa]	509.41	468.55	468.85	482.42	509.40[ab]	518.21[ab]

[a] Ref. 8. [b] Ref. 1, 3 and 8. [c] Ref. 1 and 5. [d] Ref. 16. [e] Ref. 17. [f] Molecular formula. [g] Formula weight. [h] Oxygen balance (based on CO). [i] Oxygen balance (based on CO_2). [j] Oxygen content in %. [k] Nitrogen and oxygen contents in %. [l] Calculated enthalpy of formation. [m] Measured densities, gas pycnometer at 25 °C. [n] Thermal decomposition temperature (onset) under nitrogen gas (DSC, 5 °C min^{-1}). [o] Calculated detonation velocity. [p] Calculated detonation pressure. [q] Heat of detonation. [r] Impact sensitivity. [s] Friction sensitivity. [t] Bond dissociation energies of trigger bond. [u] Φ_{H-L} = HOMO–LUMO energy gaps. [v] I_{sp} = specific impulse of neat compound. [w] ρI_{sp} = density specific impulse of neat compound. [x] Characteristic velocity. [y] I_{sp} = specific impulse at 88% compound and 12% Al. [z] ρI_{sp} = density specific impulse at 88% compound and 12% Al. [aa] Specific impulse were calculated at ambient pressure of 0.1 MPa, chamber pressure of 7 MPa, an isobaric pressure of 70 bar and initial temperature of 3300 K. [ab] This work.

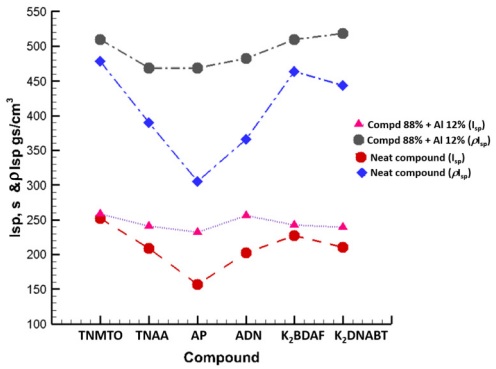

Fig. 3 Comparison of propulsive properties.

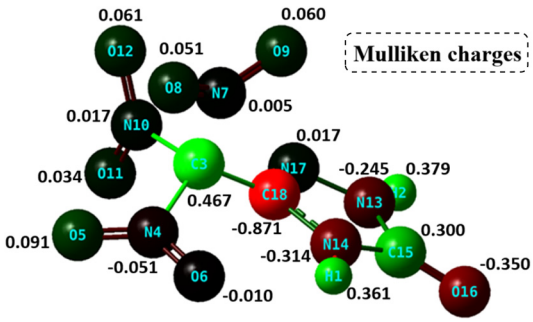

Fig. 4 Mulliken charges on **TNMTO**, **6**.

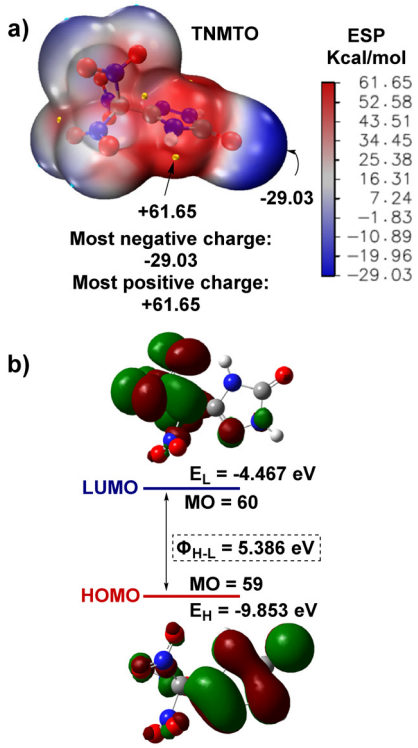

Fig. 5 (a) Electrostatic potential (ESP) maps of **TNMTO**, **6**. (b) HOMO–LUMO molecular orbitals.

in less sensitivity. The ratio of negative surface area for **TNMTO** was calculated to be 50.10, and that is higher than NTO (47.38), RDX (44.26) and TNT (42.12) (see Table S3, ESI†). Based on the balance of charges, the stability order is HMX > RDX > TNT > NTO > **TNMTO** (see Table S3, ESI†). The kinetic stability of **TNMTO** was predicted as HOMO and LUMO energy gaps, and order of kinetic stabilities is **TNMTO** < TNAA < TNT < RDX < HMX.

Furthermore, the relationship between the quantum mechanical electron density (ρ) and reduced density gradient ($s = 0.5(3\pi^2)^{1/3}|\nabla\rho|/\rho^{4/3}$ for **TNMTO** was obtained and shown as noncovalent interaction (NCl) plots. Where, reduced density gradient spikes at zero, negative and positive density values of sign $(\lambda^2)\rho(r)$ signify the van der Waals (VDW) interactions, H-bond interactions, steric effect, respectively (Fig. 6). Most of these close contacts are in the range of 2.770 Å to 2.988 Å, confirming the presence of van der Waals (VDW) interactions and H-bond interactions in the molecule.

The stability of **TNMTO** crystals is supported by various types of interactions (O–O (40.5%), O–N (20.2%) and O–H (30.0%)), which revealed with the help of Hirshfeld surfaces analysis (calculated with CrystalExplorer 21.5 software),[21] as shown in Fig. 7.

The thermal stabilities of the new compounds were measured at two different heating rates (5 °C min^{-1} and 10 °C min^{-1}) using DSC and TGA (see Fig. S26–S42, ESI†) and the results are also agreed supported with their bond dissociation

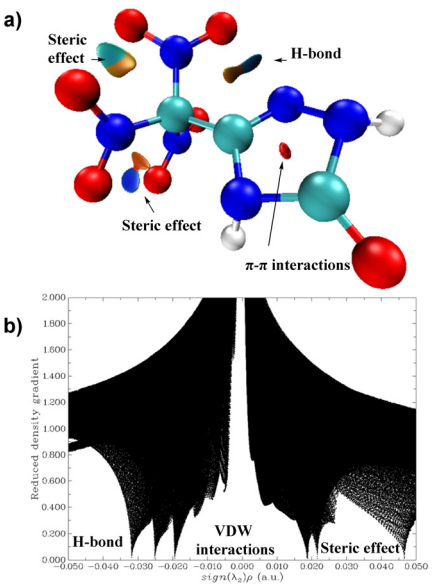

Fig. 6 Non-covalent interaction (NCI): (a) reduced density gradient (RDG) and (b) scatter diagram of compound **TNMTO**, **6** at B3LYP/6-311++G(d,p) level.

energies (BDEs) (Table 1). The bond dissociation energies (BDEs) of the trigger bond of **TNMTO** is 58.15 kJ mol^{-1} which is significantly lower than that of TNAA (102.11 kJ mol^{-1}) (Table 1). **TNMTO** is solid at room temperature and decom-

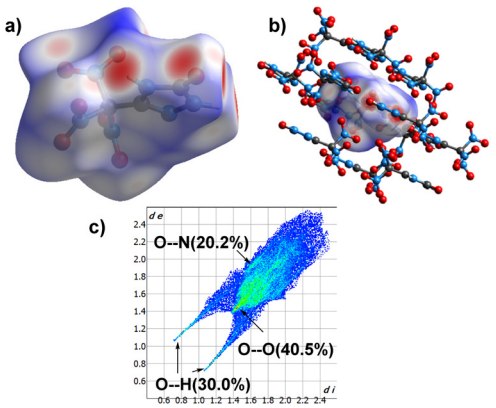

Fig. 7 (a) Hirshfeld surfaces in crystal stacking for compound **TNMTO**, **6**. (b) Arrangement in crystal packing. (c) 2D-fingerprint and individual contribution of major close contacts.

poses at 80 °C on heating without melting (see Fig. S26, ESI†). The mechanical stabilities of **TNMTO** were determined by measuring their friction sensitivities (FS) and impact sensitivities (IS) using friction tester and BAM drop hammer techniques[22] and found to be 10 J and 120 N, respectively, which are comparable to RDX (120 N). These indicate that **TNMTO** is more stable than ADN (IS = 3–5 J and FS = 64–72 N).

Detonation properties of **TNMTO** were estimated by using the EXPLO5 program (v. 6.06).[19] **TNMTO** exhibits superior detonation properties (P = 35.01 GPa, D = 8997 ms^{-1}) than RDX (P = 34.07 GPa, D = 8867 ms^{-1}), TNAA (P = 23.00 GPa, D = 7503 ms^{-1}), ADN (P = 23.60 GPa, D = 7860 ms^{-1}), K_2BDAF (P = 30.10 GPa, D = 8138 ms^{-1}), K_2DNABT (P = 31.70 GPa, D = 8330 ms^{-1}), and AP (P = 15.80 GPa, D = 6368 ms^{-1}). The heat of detonation (Q, energy) and characteristic velocity (C^*, efficacy) of **TNMTO** ($-Q$ = 5626 kJ kg^{-1}, C^* = 1501 ms^{-1}) are significantly higher than TNAA ($-Q$ = 3215 kJ kg^{-1}, C^* = 1289 ms^{-1}, AP ($-Q$ = 1435 kJ kg^{-1}, C^* = 977 ms^{-1}), ADN ($-Q$ = 2754 kJ kg^{-1}, C^* = 1267 ms^{-1}), K_2BDAF ($-Q$ = 5514 kJ kg^{-1}, C^* = 1267 ms^{-1}) and K_2DNABT ($-Q$ = 4959 kJ kg^{-1}, C^* = 1267 ms^{-1}) (Table 1, Fig. S45 and 46, ESI†).

3. Conclusion

A scalable synthesis of **TNMTO** has been developed. **TNMTO** was fully characterized by various techniques such as FTIR, NMR, elemental analysis and single crystal X-ray analysis. This new compound exhibits a very high density (1.90 g cm^{-3}), supported by intermolecular H-bonds and π–π-interactions. However, the cyclic urea moiety makes it more hygroscopic. Based on calculated detonation properties (P = 35.01 GPa, D = 8997 ms^{-1}) and ballistic properties ($I_{sp(neat)}$ = 251.85 s, $\rho I_{sp(neat)}$ = 478.52 gs cm^{-3}, $C^*_{(neat)}$ = 1501 ms^{-1}), it has potential to replace AP and ADN as a green oxidizer in solid rocket propulsion. **TNMTO** exhibits greater stability toward mechanical stimuli and comparably lower thermal stability than ADN.

Author contributions

S. L. investigation, methodology, conceptualization and manuscript writing. R. J. S. X-ray data collection and structure solving. S. L. and J. M. S. conceptualization, manuscript writing – review and editing, supervision.

Conflicts of interest

The authors declare no competing financial interest.

Acknowledgements

The Rigaku Synergy S Diffractometer was purchased with support from the National Science Foundation MRI program (1919565). We are grateful for the support of the Fluorine-19 fund.

References

1 (*a*) J. P. Agrawal and R. D. Hodgson, *Organic chemistry of explosives*, John Wiley & Sons, Ltd, Chichester, 2007, p. 243; (*b*) S. Lal, R. J. Staples and J. M. Shreeve, FOX-7 based nitrogen rich green energetic salts: Synthesis, characterization, propulsive and detonation performance, *Chem. Eng. J.*, 2023, **452**, 139600.

2 (*a*) N. Kubota, Propellants and explosives, in *Thermochemical aspects of combustion*, Wiley-VCH, Weinheim, 2nd edn, 2006; (*b*) S. Lal, R. J. Staples and J. M. Shreeve, FOX-7 derived nitramines: Novel propellants and oxidizers for solid rocket propulsion, *Chem. Eng. J.*, 2023, **468**, 143737; (*c*) T. M. Klapötke, *Chemistry of high-energy materials*, De Gruyter, Berlin, 2nd edn, 2012.

3 (*a*) H. Vogt, J. Balej, J. E. Bennett, P. Wintzer, S. A. Sheikh and P. Gallone, *Ullmann's Encyclopedia of Industrial Chemistry*, Wiley-VCH, 2002; (*b*) J. P. Agrawal, *High Energy Materials: Propellants, Explosives and Pyrotechnics*, Wiley-VCH, Weinheim, 1st edn, 2010; (*c*) N. Yedukondalu and G. Vaitheeswaran, Polymorphism, phase transition, and lattice dynamics of energetic oxidizer ammonium perchlorate under high pressure, *J. Phys. Chem. C*, 2019, **123**, 2114–2126.

4 F. P. Madyakin, *Components and combustion products of pyrotechnic compositions*,KGTU, Kazan, 2006, vol. 1.

5 G. Zhao, P. Yin, D. Kumar, G. H. Imler, D. A. Parrish and J. M. Shreeve, Bis(3-nitro-1-(trinitromethyl) 1*H* 1,2,4-triazol-5-yl)-methanone: An applicable and very dense green oxidizer, *J. Am. Chem. Soc.*, 2019, **141**, 19581–19584.

6 I. L. Dalinger, K. Y. Suponitsky, T. K. Shkineva, D. B. Lempert and A. B. Sheremetev, Bipyrazole bearing ten nitro groups: A novel highly dense oxidizer for forward-looking rocket propulsions, *J. Mater. Chem. A*, 2018, **6**, 14780–14786.

7 H. Gao and J. M. Shreeve, The many faces of FOX-7: A precursor to high-performance energetic materials, *Angew. Chem., Int. Ed.*, 2015, **54**, 6335–6338.
8 T. T. Vo, D. A. Parrish and J. M. Shreeve, Tetranitroacetimidic acid: A high oxygen oxidizer and potential replacement for ammonium perchlorate, *J. Am. Chem. Soc.*, 2014, **136**, 11934–11937.
9 S. Lal, R. J. Staples and J. M. Shreeve, Design and synthesis of high-performance planar explosives and solid propellants with tetrazole moieties, *Org. Lett.*, 2023, **25**, 5100–5104.
10 (*a*) N. Wingborg, Ammonium dinitramide-water: Interaction and properties, *J. Chem. Eng. Data*, 2006, **51**, 1582–1586; (*b*) N. Yedukondalu, V. D. Ghule and G. Vaitheeswaran, High pressure structural, elastic and vibrational properties of green energetic oxidizer ammonium dinitramide, *J. Chem. Phys.*, 2016, **145**, 064706; (*c*) F.-Y. Chen, C.-L. Xuan, Q.-Q. Lu, L. Xiao, J.-Q. Yang, Y.-B. Hu, G.-P. Zhang, Y.-L. Wang, F.-Q. Zhao, G.-Z. Hao and W. Jiang, A review on the high energy oxidizer ammonium dinitramide: Its synthesis, thermal decomposition, hygroscopicity, and application in energetic materials, *Def. Technol.*, 2023, **19**, 163–195.
11 (*a*) W. Hunter, The production of tertranitromethane and nitroform, B.I.O.S. final report No. 709, item no. 22, British Intelligence Objectives Sub-committee, London, 1946; (*b*) M. B. Frankel, F. C. Gunderloy and D. O. Woolery II, *US Patent*, 1978, **4**, 122–124; (*c*) P. S. Dendage, D. B. Sarwade, S. N. Asthana and H. Singh, Hydrazinium nitroformate (HNF) and HNF based propellants: A review, *J. Energ. Mater.*, 2001, **19**, 41–78.
12 (*a*) K.-Y. Lee and M. D. Coburn, 3-Nitro-1,2,4-triazol-5-one, A less sensitive explosive, *U.S. Patent*, 1988, **4**, 733; (*b*) R. R. Sirach and P. N. Dave, 3-Nitro-1,2,4-triazol-5-one (NTO): high explosive insensitive energetic material, *Chem. Heterocycl. Compd.*, 2021, **57**, 720–730.
13 (*a*) J. Zhang, Q. Zhang, T. T. Vo, D. A. Parrish and J. M. Shreeve, Energetic salts with π-stacking and hydrogen-bonding interactions lead the way to future energetic materials, *J. Am. Chem. Soc.*, 2015, **137**, 1697–1704; (*b*) J. Zhang, J. Zhang, D. A. Parrish and J. M. Shreeve, Desensitization of the dinitromethyl group: molecular/crystalline factors that affect the sensitivities of energetic materials, *J. Mater. Chem. A*, 2018, **6**, 22705–22712.
14 A. A. Astrat'ev, D. V. Dashko, A. Y. Mershin, A. I. Stepanov and N. A. Urazgil'deev, *Russ. J. Org. Chem.*, 2001, **37**, 729–733.
15 J. Bellamy, *FOX-7 (1,1-Diamino-2,2-dinitroethene). In high energy density materials*, Springer, Berlin, Heidelberg, 2007, pp. 1–33.
16 (*a*) Y. Tang, C. He, L. A. Mitchell, D. A. Parrish and J. M. Shreeve, Potassium4,4″-bis(dinitromethyl)-3,3″-azofurazanate: A highly energetic 3D-metal organic framework as a promising primary explosive, *Angew. Chem., Int. Ed.*, 2016, **55**, 5565–5567; (*b*) E. N. Rao and G. Vaitheeswaran, Structure-property correlation studies of potassium 4,4′-bis(dinitromethyl)-3,3′-azofurazanate: A noncentrosymmetric primary explosive, *J. Phys. Chem. C*, 2019, **123**, 10034–10050.
17 D. Fischer, T. M. Klapötke and J. Stierstorfer, Potassium 1,1′-Dinitramino-5,5′-bistetrazolate: A primary explosive with fast detonation and high initiation power, *Angew. Chem., Int. Ed.*, 2014, **53**, 8172–8175.
18 M. J. Frisch, G. W. Trucks, H. B. Schlegel, G. E. Scuseria, *et al.*, *Revision D.01 ed*, Gaussian, Inc., Wallingford, CT, 2003.
19 EXPLO5; OZM Research s.r.o.: Hrŏchuv Tŷnec, Czech Republic. **https://www.ozm.cz/explosives-performance-tests/thermochemical-computer-code-explo5/**(accessedon 2022-10-20).
20 T. Lu and F. Chen, Multiwfn: A multifunctional wavefunction analyzer, *J. Comput. Chem.*, 2012, **33**, 580–592.
21 P. R. Spackman, M. J. Turner, J. J. McKinnon, S. K. Wolff, D. J. Grimwood, D. Jayatilaka and M. A. Spackman, CrystalExplorer: A program for Hirshfeld surface analysis, visualization and quantitative analysis of molecular crystals, *J. Appl. Crystallogr.*, 2021, **54**, 1006–1011.
22 (*a*) A 25 mg sample was subjected to a drop-hammer test with a 5 or 10 kg dropping weight. The impact sensitivity was characterized according to the UN recommendations (insensitive, >40 J; less sensitive, 35 J; sensitive, 4 J; very sensitive, 3 J) (*b*) NATO, Standardization Agreement 4487 (STANAG 4487), Explosives, Friction Sensitivity Tests, 2002; (*c*) (i) United Nations. Recommendations On the Transport of Dangerous Goods. Manual of Tests and Criteria, 7th revised ed., 2019; BAM Fallhammer, p 85; 13.4.2 Test code 3 (a) (ii); and BAM friction apparatus, p 117; 13.5.1 Test code 3 (b) (i).